Assessment of a New Analytical Expression for the Maximum-Power Point Voltage with Series Resistance

Alfredo Sanchez Garcia, Sissel Tind Kristensen, and Rune Strandberg
University of Agder, Grimstad, 4879, Norway

Abstract

This work compares a recently developed analytical expression for the maximum-power point voltage with experimental data, to test its usability for crystalline silicon solar cells. The experimental data covers measurements from 18 multicrystalline silicon solar cells with different bulk resistivities and cell architectures. We show that the expression is able to predict the maximum power obtainable by the measured cells with relative discrepancies below 1%. Additionally, we compare the accuracy of this new expression with two already existing models.

1 Introduction

The maximum-power point of solar cells that follow Shockley's diode equation has been studied from an analytical perspective in a number of works, such as Refs. [1] and [2]. There, the authors showed that Lambert's W function [3] allowed for a simple analytical expression of the maximum-power point voltage, V_{mpp}, and, consequently the maximum-power point current and power, i_{mpp} and P_{mpp}, respectively.

Some work has been done aiming to quantify analytically the effect of series resistance on various solar cell parameters [4, 5, 6, 7]. Particularly in Ref. [6], Singal obtained an approximate closed-form expression of V_{mpp} in terms of the open-circuit voltage, V_{oc}.

Recently, a new expression for V_{mpp} that accounts for the effect of series resistance, and is comparable in simplicity to the expression derived by Khanna in Ref. [1], has been derived and tested against a numeric one-diode model for a number of different bandgaps [8].

In this paper, we aim to test the applicability of this new expression for V_{mpp} in crystalline silicon (c-Si) solar cells. The current-voltage (I-V) characteristics of 18 compensated multicrystalline silicon (mc-Si) solar cells, as well as the series resistance and sample characteristics, were measured at various temperatures. We compare the measured values of V_{mpp}, i_{mpp} and P_{mpp} of the measured cells to their corresponding counter parts predicted by the expression derived in Ref. [8]. Additionally, we test the accuracy of the expressions derived in Ref. [8] against Singal's expressions (Ref. [6]) and a numerical model.

2 Theoretical Framework

When series resistance is accounted for in Shockley's diode equation [9], the total current, i, produced by a solar cell is given by [10]

$$i = i_{\mathrm{G}} - i_0 \exp\left(\frac{V + iR}{V_{\mathrm{t}}}\right) \tag{1}$$

where i_{G} and i_0 are the generation and the thermal recombination [11] currents, respectively; V is the voltage and $qV_{\mathrm{t}} = kT$ with q and k being the elementary charge and Boltzmann's constant; and R is the series resistance. Banwell et al. showed in Ref. [4], that Lambert's W function, defined by $x = \mathrm{W}(xe^x)$ allows for Eq. (1) to be expressed in closed-form as

$$i = i_{\mathrm{sc}} - \frac{V_t}{R}\mathrm{W}\left(\frac{i_{\mathrm{sc}}R}{V_{\mathrm{t}}}\exp\left[\frac{V}{V_{\mathrm{t}}} - \frac{V_{\mathrm{oc}}}{V_{\mathrm{t}}} + \frac{i_{\mathrm{sc}}R}{V_{\mathrm{t}}}\right]\right), \tag{2}$$

where we have approximated i_{G} by i_{sc} and made use of the identity $i_0 = i_{\mathrm{sc}}/\exp\left({}^{V_{\mathrm{oc}}}/_{V_{\mathrm{t}}}\right)$. The latter follows from Eq. (1) by noting that $i(V_{\mathrm{oc}}) = 0$ [10].

At the maximum-power point, it holds that ${}^{\mathrm{d}P}/_{\mathrm{d}V} = 0$, with P being given by the product $P = i \cdot V$. Inserting Eq. (2) results into an transcendental equation in V that does not have an analytical solution and needs to be solved numerically. However, some approximate analytical solutions can be found in the literature.

2.1 Without Lambert's W function

Already in 1981, Singal derived in Ref. [6] approximate analytical expressions for V_{mpp}, i_{mpp} and P_{mpp}. In his derivation, Singal did not make use of Lambert's W function. Instead, he noted that, for most solar cells, $V_{\mathrm{oc}} >> V_{\mathrm{t}}$, which allowed him to take a series of approximations that converted the transcendental problem into

an analytically solvable equation. The proposed expressions for the maximum-power point were

$$V_{\mathrm{mpp}} = V_{\mathrm{oc}} \left[1 - \frac{1}{v} \log(1 + f(v)) + \frac{1}{v} \log \left(1 + \frac{2 i_{\mathrm{sc}} R}{V_{\mathrm{oc}}} \frac{v f(v)}{(1 + f(v))^2} \right) \right.$$

$$\left. - \frac{i_{\mathrm{sc}} R}{V_{\mathrm{oc}}} \frac{f(v)}{1 + f(v)} + \left(\frac{i_{\mathrm{sc}} R}{V_{\mathrm{oc}}} \right)^2 \frac{2 v f(v)}{(1 + f(v))^3} \right], \quad (3)$$

$$i_{\mathrm{mpp}} = i_{\mathrm{sc}} \left[1 - \frac{1}{1 + f(v)} - \frac{2 i_{\mathrm{sc}} R}{V_{\mathrm{oc}}} \frac{v f(v)}{(1 + f(v))^3} \right], \quad (4)$$

where $v = {}^{V_{\mathrm{oc}}}/_{V_{\mathrm{t}}}$ and $f(v) = v - \log(v)$. The corresponding expression for P_{mpp} is obtained by multiplying Eqs. (3) and (4).

2.2 With Lambert's W function

Sanchez and Strandberg showed in Ref. [8] that approximating Lambert's W function by its argument in the derivation of V_{mpp} allowed for an approximate analytical solution of the transcendental problem. The obtained expression was

$$V_{\mathrm{mpp}} = i_{\mathrm{sc}} R + V_{\mathrm{t}} \left(\mathrm{W} \left[\exp \left[1 + \frac{V_{\mathrm{oc}}}{V_{\mathrm{t}}} - 2 \frac{i_{\mathrm{sc}} R}{V_{\mathrm{t}}} \right] \right] - 1 \right). \quad (5)$$

From Eq. (2), it is possible to calculate the maximum-power point current, i_{mpp}, and power, P_{mpp}, by inserting Eq. (5) into Eq. (2) and then calculating the product $i_{\mathrm{mpp}} \cdot V_{\mathrm{mpp}}$. The authors in Ref. [8] also proposed two approximate expressions for these quantities,

$$i_{\mathrm{mpp}} = i_{\mathrm{sc}} \left(1 - \frac{1}{\mathrm{W}\left[\alpha(R)\right]} \right), \quad (6)$$

$$P_{\mathrm{mpp}} = i_{\mathrm{sc}}^2 R \left(1 - \frac{1}{\mathrm{W}\left[\alpha(R)\right]} \right) + i_{\mathrm{sc}} V_{\mathrm{t}} \left(\mathrm{W}\left[\alpha(R)\right] - 2 + \frac{1}{\mathrm{W}\left[\alpha(R)\right]} \right), \quad (7)$$

where $\alpha(R)$ equals the argument of Lambert's W function in Eq. (5).

2.3 The ideality factor

Foreseeing its usability in the comparison with our experiments, it is worth dedicating a section to the ideality factor, n. At the beginning of this section, we introduced the recombination term of the diode equation as $i_0 \exp\left[{}^{V}/_{V_\mathrm{t}}\right]$. This is true only for solar cells that follow the ideal diode equation, which assumes that all recombination occurs in the cell bulk through band-to-band transitions or through Shockley-Read-Hall (SRH) recombination. Real cells experience other types of recombination and, also, in different areas of the device [10]. In order to account for these, we need to introduce an ideality factor, n, in the exponent as $qV_\mathrm{t} \to qnV_\mathrm{t} = nkT$. The ideality factor is then a measure of how ideal the cell in question is [10].

The ideality factor of a cell may be extracted from the experimental data by fitting the obtained $I-V$ characteristics to Shockley's diode equation. Let us instead propose an alternative method that requires less computational power. From Eq. (1), we can solve for nV_t and obtain

$$nV_\mathrm{t} = \frac{V + iR - V_\mathrm{oc}}{\log\left(1 - \frac{i}{i_\mathrm{sc}}\right)}. \tag{8}$$

Here, we have also approximated i_G by i_sc and made use of $i_0 = i_\mathrm{sc}/\exp\left({}^{V_\mathrm{oc}}/_{V_\mathrm{t}}\right)$. Eq. (8) is only defined in the real axis within the interval $0 < i < i_\mathrm{sc}$, i.e., for all points in the $I - V$ curve except V_oc and i_sc. Assuming that the ideality factor is constant throughout the $I - V$ characteristic, we can evaluate Eq. (8) at the maximum-power point and express n as

$$n = \frac{q}{kT}\frac{V_\mathrm{mpp} + i_\mathrm{mpp}R - V_\mathrm{oc}}{\log\left(1 - \frac{i_\mathrm{mpp}}{i_\mathrm{sc}}\right)}. \tag{9}$$

All the physical quantities appearing in Eq. (9) can be extracted from the measurements, which allows for the determination of n at different temperatures.

In Ref. [12], Townsend proposed a method for estimating the performance of coupled photovoltaic systems. To this end, he compared various models that could be potential candidates. It is worth mentioning that Townsend arrived at Eq. (9) when obtaining a solution for what he denoted the "Lumped, 1 Mechanism with 4 Parameters" model [12].

3 Experimental Method

To compare the analytical expression with experimental data, 18 compensated p-type mc-Si solar cells were studied. The cells were fabricated from three different

ingots with different bulk resistivities, ρ, and different cell architectures. The cells can be divided into three groups: (a) $\rho = 0.5\ \Omega \cdot \mathrm{cm}$, Passivated Emitter Rear Cells (PERC), (b) $\rho = 1.3\ \Omega \cdot \mathrm{cm}$, PERC, and (c) $\rho = 1.3\ \Omega \cdot \mathrm{cm}$, Aluminum Back Surface Field (Al-BSF) cells. Each group contains six cells from various brick positions, numbered from 001-060, with position 001 at the bottom of the brick and position 060 at the top. The measurements were performed using a NeonSee$^{\mathrm{TM}}$ AAA Sun simulator, enabling acquisition of the $I - V$ characteristics of the cells, as well as the series resistance, at various temperatures ranging from 293 K to 343 K. The cell temperature was controlled using a built-in water heater.

4 Numerical Method

We denote with the label "exp", the experimental values of V_{mpp}, i_{mpp} and P_{mpp}. The experimental values of V_{oc}, i_{sc} and R are used as inputs to evaluate Eqs. (5), (6) and (7) to calculate V_{mpp}, i_{mpp} and P_{mpp} at multiple temperatures. We denote these with the label "mod". Singal's model, i.e., Eqs. (3), (4) and the corresponding P_{mpp}, will be labeled "S". As all the expressions presented in sections 2.1 and 2.2 result from approximations, it may also be of interest to compare the experiments with the value of V_{mpp}, i_{mpp} and P_{mpp} that we can obtain directly from Eq. (2). To do so, we calculate values of V_{mpp} by finding numerically the voltage that maximizes $P = Vi$, with i being given by Eq. (2). In order to do this, we first make use of experimental values of V_{oc}, i_{sc} and R and insert them in Eq. (2). We then make use of an auxiliary function, $f(V) = -Vi$, and find the voltage that minimizes it. We denote by $V_{\mathrm{mpp}}^{\mathrm{num}}$, the values of V_{mpp} obtained in this way. The corresponding i_{mpp} and P_{mpp} are also denoted by the label "num".

4.1 Simultaneous determination of the ideality factor and the series resistance

Before we compare with the experiments, we need to address the way R is obtained from the experimental $I - V$ characteristics. In our case, the NeonSee$^{\mathrm{TM}}$ AAA Sun simulator software estimates the value of the series resistance from the $I - V$ characteristics by computing the negative reciprocal of the slope at $V = V_{\mathrm{oc}}$. As noted in, e.g., Ref. [12], this method overestimates the value of R. This can be analytically shown from Eq. (1) by taking the derivative of i with respect to V,

evaluating at $V = V_{\rm oc}$ and solving for R. We obtain

$$R = -\frac{1}{\left.\frac{\partial i}{\partial V}\right|_{V=V_{\rm oc}}} - \frac{1}{\frac{qi_0}{nkT}\exp\left[\frac{qV_{\rm oc}}{nkT}\right]} = R_0 - \frac{nkT}{qi_{\rm sc}}, \tag{10}$$

where we have introduced R_0 as the estimate of the R that the software gives and again made use of the identity $i_0 = i_{\rm sc}/\exp\left({}^{V_{\rm oc}}/_{nV_{\rm t}}\right)$. From Eq. (10), we note that R is always going to be smaller than the given estimate, R_0 [12].

In order to being able to compare with the experiments, we need to not only accurately estimate R but also n. A straightforward method would be to extract these parameters from the measured $I-V$ characteristics by, e.g., least-square fitting the data points to Eq. (1). Alternatively, we can note from Eqs. (9) and (10) that we have $n(R)$ and $R(n)$, respectively. Solving the system of equations in closed-form yields

$$n = \frac{q}{kT}\frac{i_{\rm sc}}{i_{\rm mpp}}\frac{i_{\rm mpp}R_0 + V_{\rm mpp} - V_{\rm oc}}{\left(1 + \frac{i_{\rm sc}}{i_{\rm mpp}}\log\left[1 - \frac{i_{\rm mpp}}{i_{\rm sc}}\right]\right)}, \tag{11}$$

$$R = -\frac{V_{\rm mpp} - V_{\rm oc} - i_{\rm sc}R_0\log\left[1 - \frac{i_{\rm mpp}}{i_{\rm sc}}\right]}{i_{\rm mpp} + i_{\rm sc}\log\left[1 - \frac{i_{\rm mpp}}{i_{\rm sc}}\right]}, \tag{12}$$

which again requires less computational power.

As a final note, it is worth pointing out that the NeonSee$^{\rm TM}$ AAA sun simulator software has been updated since these measurements were obtained and now the "Variable Intensity Method" is used to extract the series resistance from the $I-V$ curves [13].

5 Numerical Results and Discussion

In Figs. 1, 2 and 3, we display $V_{\rm mpp}$, $i_{\rm mpp}$, and $P_{\rm mpp}$, respectively, as a function of the cell temperature. The values correspond to the cell in brick position 012 of group (a). In all three figures, the experimental values of the corresponding parameters are represented with blue crosses. The values corresponding to the numerical model are represented with continuous black lines. The "mod" parameters, i.e., Eqs. (5), (6) and (7), are represented with continuous gray lines. Finally, Singal's model, i.e.,

Eqs. (3) and (4), is represented with dashed red lines. In all three figures, it is assumed an ideality factor of 1 in both the numerical and the analytical models.

Starting with Fig. 1, we see that the values of $V_{\mathrm{mpp}}^{\mathrm{num}}$ and both the approximate analytical models overlap well, but all three models appear to underestimate $V_{\mathrm{mpp}}^{\mathrm{exp}}$ by 3.5%, on average. As for Fig. 2, we we see that the numerical and the analytical models overlap well, but overestimate the experimental values of i_{mpp}. Since there is a good agreement between the "num", "mod" and "S" V_{mpp} and i_{mpp} values, we also find a good agreement between $P_{\mathrm{mpp}}^{\mathrm{mod}}$, $P_{\mathrm{mpp}}^{\mathrm{S}}$ and $P_{\mathrm{mpp}}^{\mathrm{num}}$, as we can see in Fig. 3. All three methods appear however to underestimate the experimental values.

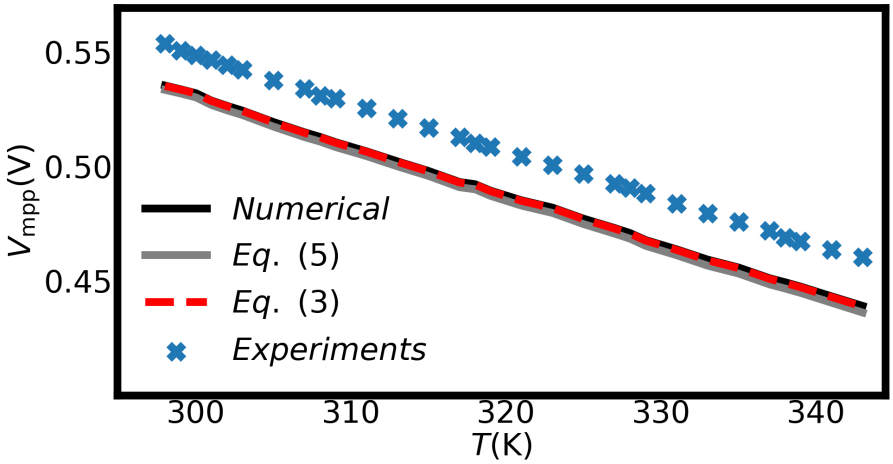

Figure 1: V_{mpp} as a function of the temperature for the cell from brick position 012 in group (a). The experimental values are represented with blue crosses. The numerical model, corresponding to $V_{\mathrm{mpp}}^{\mathrm{num}}$ in section 4, is represented by continuous black lines. The analytical models, corresponding to Eqs. (3) and (5), are represented by dashed red and continuous gray lines, respectively.

5.1 The effect of the ideality factor

Understandingly, we may find discrepancies between the experiments and both analytical models, as the latter result from approximations of the numerical model. But one would expect the numerical model to accurately describe the experiments as it is derived from the (modified) diode equation, Eq. (1).

One possible reason for the mismatch between the models and the experiments is the ideality factor of the measured cells. To compute Figs. 1, 2 and 3, we have

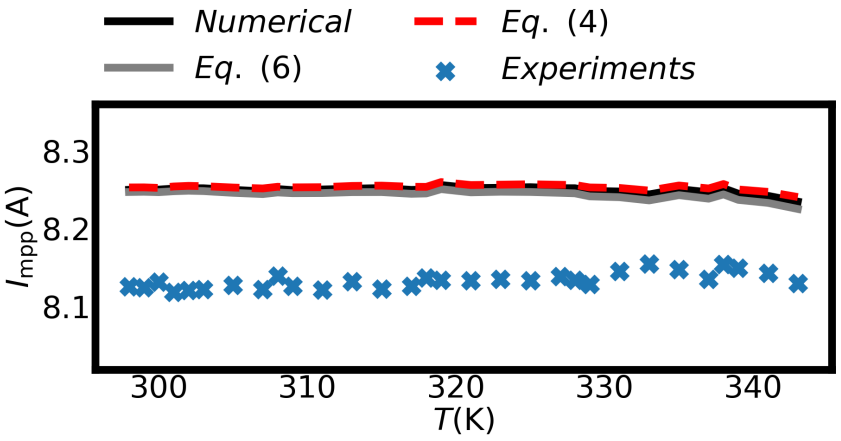

Figure 2: i_{mpp} as a function of the temperature for the cell in position 012 in group (a).

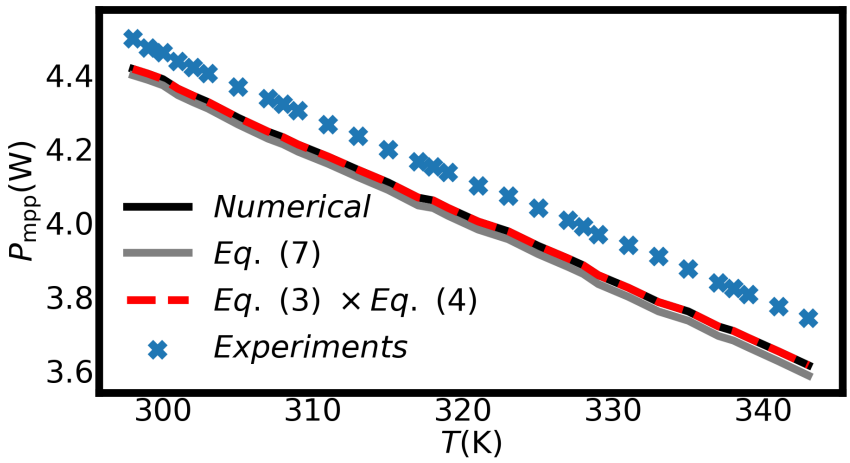

Figure 3: P_{mpp} as a function of the temperature for the cell from brick position 012 in group (a).

assumed $n = 1$ which, as noted in section 2.3, is only true for solar cells that follow the ideal diode equation. Indeed, the measured cells do not behave like ideal diodes. To see this, we display in Fig. 4 the $I - V$ characteristics corresponding to the cell from brick position 005 of group (c) at $T = 298$ K (black dots), as well as three simulated cases where the ideality factor was obtained using different methods: (i, in blue) by fitting the experimental $I - V$ curve to Shockley's diode equation (Eq. (1)

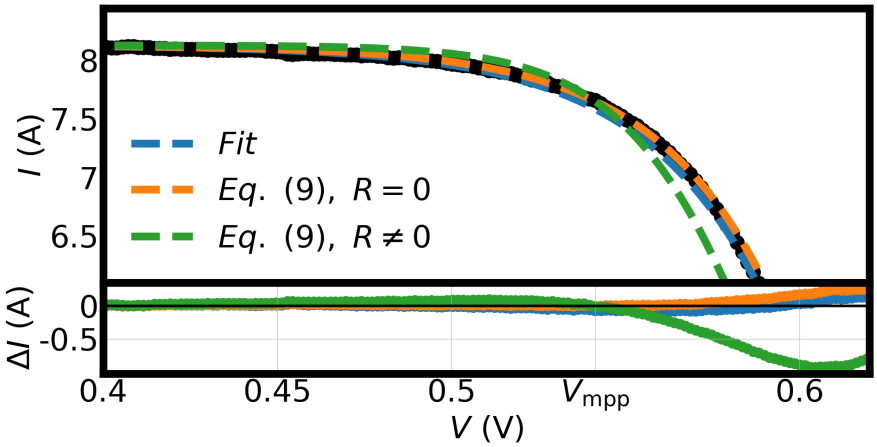

Figure 4: $I-V$ characteristics corresponding to cell from brick position 005 of group (c) at $T = 298$ K. The experimental values are represented with black dots. The dashed blue line is obtained by evaluating Shockley's single diode equation (Eq. (1) with $R = 0$) with the measured voltages and an ideality factor obtained from a least-square fit. The orange dashed line is also obtained from the single diode equation but evaluated with an ideality factor obtained from Eq. (9), setting $R = 0$. Finally, the green dashed line is obtained by evaluating Eq. (2) with the measured voltages and an ideality factor obtained from Eq. (9) with the measured values of the series resistance, R_0. At the bottom, we display a residual plot.

with $R = 0$) and extracting n from the fit, (ii, in orange) by evaluating Eq. (9) with $R = 0$ and the experimental values of $V_{\rm oc}$, $i_{\rm sc}$, $V_{\rm mpp}$ and $i_{\rm mpp}$ corresponding to the displayed $I-V$ curve and (iii, in green) by evaluating Eq. (9) with $R = R_0$ (the series resistance value provided by the Sun simulator software) and the experimental values of $V_{\rm oc}$, $i_{\rm sc}$, $V_{\rm mpp}$ and $i_{\rm mpp}$. At the bottom of Fig. 4, we display the corresponding residual plot, i.e., a plot of the difference between the models and the obtained experimental values. The obtained ideality factor is different from one in all three represented cases; 1.37 and 1.32 for methods (i) and (ii), respectively and 0.80 for method (iii).

In Fig. 5, we display the relative discrepancy between the experimental values of $V_{\rm mpp}$ (dots) and $P_{\rm mpp}$ (crosses) and the corresponding values obtained from the analytical models for the cells in group (a) at $T = 298$ K. The "mod" parameters (Ref. [8]) are represented with the color blue and the "S" parameters (Ref. [6]), with the color red. Here, we have introduced the ideality factor of the corresponding cells calculated with Eq. (9) and the measured value of the series resistance, R_0 (method

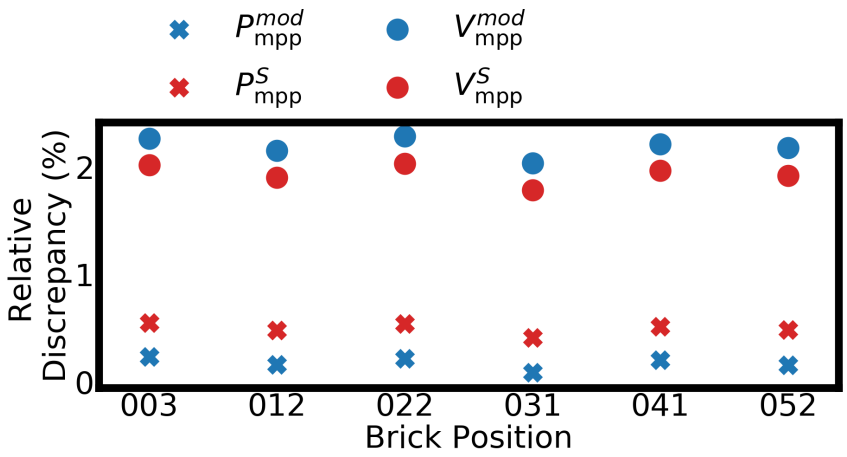

Figure 5: Relative discrepancy between the experimental and the modeled values of $V_{\rm mpp}$ (dots) and $P_{\rm mpp}$ (crosses) for all cells in group (a) and at $T = 298$ K. The Ref. [8] points correspond to the "mod" parameters, i.e., Eqs. (5) and (7). Ref. [6] points correspond to the "S" parameters; Eqs. (3) and $P^{\rm S}_{\rm mpp}$ given by Eqs. (3) $\times$ Eqs. (4). All expressions are evaluated at the series resistance provided by the Sun simulator software, R_0, and at $n(R_0)$ with n being given by Eq. (9).

(iii) above). In the case of $V_{\rm mpp}$, accounting for the ideality factor of the cells reduces the relative discrepancy between the experiments and both the numerical and the analytical models by approximately 50%. From Fig. 5, we see that both Eq. (7) and Singal's expression predict the experimental values of $P_{\rm mpp}$ for all brick positions with a relative error below 0.5% for all cells in all three groups.

5.2 Extraction of n and R

Even though we obtain a reasonable relative discrepancy with the experiments when comparing the $P_{\rm mpp}$ values, the results for $V_{\rm mpp}$ are not ideal. We can reduce the relative discrepancy between the models and the experiments by extracting R and n directly from the $I - V$ curves. As noted in section 4.1, this may be done by fitting the obtained $I - V$ characteristics to Eq. (2) or by making use of Eqs. (11) and (12). The results of this procedure are displayed in Figs. 6 and 7, where we show the relative discrepancy between the experimental values of $V_{\rm mpp}$ and $P_{\rm mpp}$ and the corresponding values obtained from the analytical models for the cells in groups (b) and (c). As it can be seen from the figures, making use of Eqs. (11) and (12) to extract n and R results in a more accurate estimation.

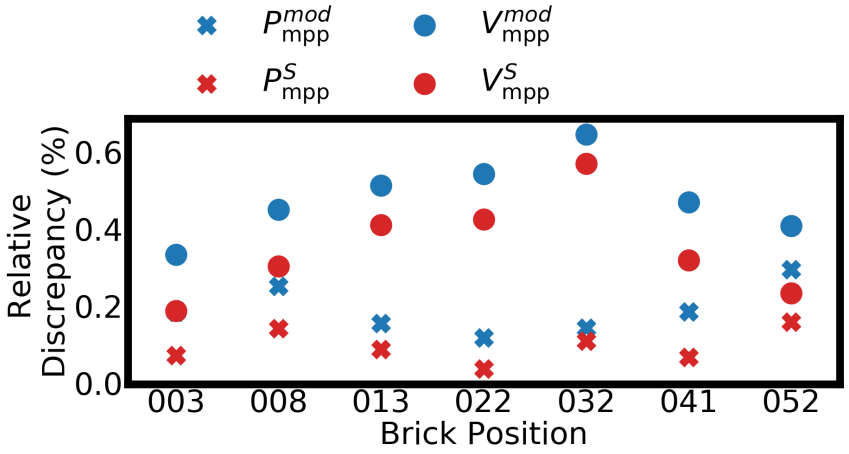

Figure 6: Relative discrepancy between the experimental and the modeled values of $V_{\rm mpp}$ (dots) and $P_{\rm mpp}$ (crosses) for all cells in group (b) and at $T = 298$ K. Here and also in Fig. 7, we have obtained n and R from Eqs. (11) and (12), respectively.

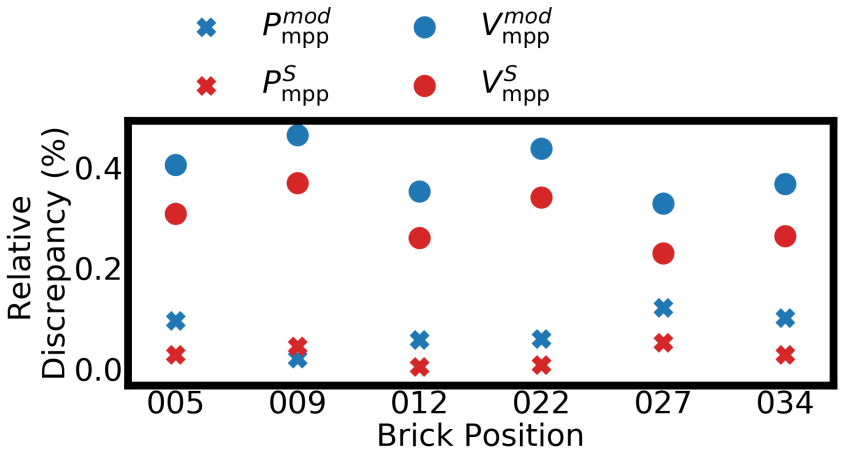

Figure 7: Relative discrepancy between the experimental and the modeled values of $V_{\rm mpp}$ (dots) and $P_{\rm mpp}$ (crosses) for all cells in group (c) and at $T = 298$ K.

Regarding the accuracy of the analytical models, we see from the figures that both models predict similar values when provided with the same input. We can therefore regard them as equally capable to predict experimental values. The main improvement that Eqs. (5), (6) and (7) may present compared to Singal's model is a simplification of the mathematical expressions.

6 Conclusion

In this work, we have tested the usability of a model for the maximum-power point, previously derived in Ref. [8], with mc-Si solar cells. To this end, we studied 18 compensated p-type mc-Si cells at multiple temperatures. To allow a comparison with the experiments we have also developed an analytical method, based on the works of Townsend in Ref. [12], that allows for the simultaneous extraction of n and R from the $I - V$ curves. We have shown that, when provided with the right input, the analytical model is able to predict experimental data with low relative discrepancy. We have also compared this new model to two already existing models; one numerical and one analytical, previously derived by Singal in Ref. [6]. Both analytical models are very similar in accuracy. The main difference between the two lies in the simplicity of the mathematical expressions. Overall, we may conclude that the model presented in Ref. [8] accurately predicts the experimental values of V_{mpp} and P_{mpp} and can be successfully applied to mc-Si solar cells.

7 Acknowledgments

A.S.G. would like to thank Martin Maier from NeonSee$^{\mathrm{TM}}$ for providing valuable information and details regarding the software employed in the Sun simulator.

References

[1] A. Khanna et al. "A fill factor loss analysis method for silicon wafer solar cells". In: *IEEE Journal of Photovoltaics* 3.4 (2013), pp. 1170–1177.

[2] A. Sergeev and K. Sablon. "Exact solution, endoreversible thermodynamics, and kinetics of the generalized Shockley-Queisser model". In: *Physical Review Applied* 10.6 (2018), p. 064001.

[3] R. M. Corless et al. "On the Lambert W function". In: *Advances in Computational Mathematics* 5.1 (1996), pp. 329–359.

[4] T. C. Banwell and A. Jayakumar. “Exact analytical solution for current flow through diode with series resistance”. In: *Electronics letters* 36.4 (2000), pp. 291–292.

[5] A. Jain and A. Kapoor. “Exact analytical solutions of the parameters of real solar cells using Lambert W-function”. In: *Solar Energy Materials and Solar Cells* 81.2 (2004), pp. 269–277.

[6] C. M. Singal. “Analytical expression for the series-resistance-dependent maximum power point and curve factor for solar cells”. In: *Solar Cells* 3.2 (1981), pp. 163–177.

[7] M. A. Green. “Accurate expressions for solar cell fill factors including series and shunt resistances”. In: *Applied physics letters* 108.8 (2016), p. 081111.

[8] A. S. Garcia and R. Strandberg. “Analytical Modeling of the Maximum-Power Point with Series Resistance”. In: *To be published.* ().

[9] W. Shockley and H. J. Queisser. “Detailed balance limit of efficiency of p-n junction solar cells”. In: *Journal of Applied Physics* 32.3 (1961), pp. 510–519.

[10] J. Nelson. *The Physics of Solar Cells*. World Scientific Publishing Company, 2003.

[11] A. Cuevas. “The recombination parameter J0”. In: *Energy Procedia* 55 (2014), pp. 53–62.

[12] T. U. Townsend. “A method for estimating the long-term performance of direct-coupled photovoltaic systems”. PhD thesis. 1989.

[13] M. Maier. *NeonSee*. Personal communication. June 8, 2021.